

# Green Synthesis and Characterization of Zinc Oxide Nanoparticles Using Neem (*Azadirachta indica* L.) Leaf Extract

K. Vignesh

Department of Plant Pathology, Palar Agricultural College, Ambur, Vellore 635 805, Tamil Nadu, India

## ABSTRACT

**Background and Objective:** Growing interest in nanotechnology is being shown in the green synthesis of metal nanoparticles using botanical extracts because it doesn't involve large energy inputs or the creation of extremely hazardous chemical by-products. The present investigation aimed to study the synthesis of zinc oxide nanoparticles synthesized from neem (*Azadirachta indica*). **Materials and Methods:** The study was conducted at the Department of Plant Pathology, Annamalai University (2023-2024). Zinc nanoparticles were synthesized using neem leaf extract, confirmed by a color change from green to dark brown. Characterization involved UV-vis spectroscopy for plasmon resonance, FESEM for surface morphology, FTIR for functional group analysis, and XRD for crystalline structure determination using the Debye-Scherrer equation. These techniques confirmed nanoparticle formation and stability. **Results:** The UV-vis absorption spectra of the synthesized zinc nanoparticles between 200-800 nm. The ZnNPs in the solution have sizes of several nm which ranged between 149.52-231.64 nm with a predominant shape cluster. Whereas, FTIR spectra of neem ZnNPs resulted in sharp absorption peaks at 3412.80, 2428.71, 2331.93, 2026.69, 1384.54, 1271.24, 872.47, 444.24  $\text{cm}^{-1}$ . The average crystalline size for neem ZnNPs was 37.00 nm. **Conclusion:** The synthesis involved combining neem extract with zinc salt under controlled stirring conditions, resulting in a color change indicating nanoparticle formation.

## KEYWORDS

Neem, zinc nanoparticles, green synthesis, UV-vis spectroscopy, FTIR analysis, Field Emission Scanning Electron Microscopy (FESEM), X-ray Diffraction (XRD)

Copyright © 2025 K. Vignesh. This is an open-access article distributed under the Creative Commons Attribution License, which permits unrestricted use, distribution and reproduction in any medium, provided the original work is properly cited.

## INTRODUCTION

Nanotechnology is a rapidly developing field that intersects with many other areas of study, particularly biology. To further advance nanotechnology, reliable and environmental friendly methods for synthesizing nanomaterials are crucial. This entails producing nanomaterials with varying biological compositions, sizes, shapes, and high monodispersity<sup>1</sup>. The importance of nanotechnology can be seen through its extensive applications in modern society. By reducing materials to the nanoscale, typically between 1-100 nm in at least one dimension, materials exhibit unique chemical, physical, magnetic, electrical and optical properties when compared to their bulk counterparts. This is due to the materials' high specific surface area on the nanoscale level.



Metal nanoparticles exhibit unique physical characteristics such as size, shape, and a larger surface area-to-volume ratio. These nanoparticles can be synthesized from various metals such as gold<sup>2</sup>, silver<sup>3</sup>, copper<sup>4</sup>, magnesium<sup>5</sup>, zinc and titanium. Among these metals, copper and zinc nanoparticles are more widely used due to their versatility in biology<sup>6</sup>. They have a broad range of antimicrobial properties but are not harmful to human health<sup>7</sup>. Zinc Oxide Nanoparticles (ZnONPs) are perfect for usage as a zinc fertilizer in plants due to their huge surface area and small size<sup>8</sup>. Ultraviolet (UV) irradiation, microwave assistance, electrochemical, sonochemical, microfluidic approach, microorganism-mediated, and plant extract-mediated techniques are some of the ways that nanoparticles can be created. Green synthesis of nanoparticles must be adopted since physical methods use energy and chemical ones involve hazardous substances. Green chemistry is supported by the creation of nanoparticles derived from plant extracts and microorganisms.

The focus of this research work was on the eco-friendly synthesis of copper and zinc nanoparticles using neem and mangrove extracts. The nanoparticles were then characterized and tested for their effectiveness against *B. maydis* under *in-vitro* conditions.

## MATERIALS AND METHODS

**Study area:** This research was conducted in the Department of Plant Pathology, Faculty of Agriculture, Annamalai University during 2023-2024.

### Synthesis and characterization of zinc nanoparticles

**Synthesis of nanoparticles from plant extract:** A mixture was prepared by combining 5 g of neem leaf powder with 150 mL of distilled water in separate beakers. Those beakers were then placed on a thermal cum magnetic stirrer for 30 min. After 30 min, the stirrer was turned off and the mixture was allowed to cool. The leaf extract was then filtered and stored in different containers. About 50 mL of distilled water was taken from a 250 mL beaker and added was 1.487 g (Zn) salt. The beaker was then placed on a thermal cum magnetic stirrer for 15 min to ensure thorough agitation of the salt. Following this, 20 mL of plant extract was added to a beaker while stirring continuously. After 30 min, a change in the color of the aqueous solution was observed. Eventually, the solution was dried and checked for sediment settling at the bottom of the container, and color change was observed. i.e., green to yellow/dark brown. A color change indicated the formation of nanoparticles. The powder was then scraped and stored in centrifuge tubes for further analysis.

### Characterization of green synthesized nanoparticles

**UV-visible spectroscopy characterization:** The reduction of silver ions was observed by analyzing the UV-vis spectrum of the reaction mixture for 24 hrs. To determine the presence of nanoparticles. In the reaction mixture, a UV-vis spectrophotometer (Shimadzu, UV-2450) was used to record the surface plasmon resonance spectra within the wavelength range of 200 to 800 nm was recorded<sup>9</sup>.

**Field Emission Scanning Electron Microscopy (FESEM) analysis:** The surface morphology of the nanocluster images was examined using a Field Emission Scanning Electron Microscope (FESEM) model JSM-7800F Schottky. The FESEM had a working distance of 6-13mm, an accelerating voltage of 5-20 keV, an emission current of 75-80 A, and provided highly magnified images ranging from 10-300,000×. The above analysis was done in the Centralised Instrumentation and Service Laboratory (CISL), Department of Physics, Annamalai University, Annamalai Nagar<sup>10</sup>.

**Fourier Transform Infrared Spectroscopy (FTIR) characterization:** The Fourier Transform Infrared Spectroscopy (FTIR) spectroscopy measurements involved analyzing the bio-transformed products found in the cell-free filtrate after 72 hrs of incubation. These products were freeze-dried and then diluted with

potassium bromide in a ratio of 1:100. The FTIR spectrum of the samples was recorded using a Nicolet 6700 spectrometer operating in the FTIR mode, with a resolution of 4 cm<sup>-1</sup>. The measurements were conducted in a range of 400 to 4000 cm<sup>-1</sup> at a resolution of 4 cm<sup>-1</sup>. Through infrared spectroscopy, the amino acids and peptides forming a protective coating around the silver nanoparticles, preventing them from agglomeration were determined<sup>10</sup>.

**X-ray diffraction (XRD) characterization:** A glass plate was immersed in a solution to create a thin layer of nanoparticle which was then used for conducting the X-ray diffraction analysis. The crystalline nanoparticles were calculated from the width of the XRD peaks and the average size of the nanoparticles can be estimated using the Debye-Scherrer equation<sup>10</sup>:

$$D = \frac{\kappa\lambda}{\beta\cos\theta}$$

Where:

D = Thickness of the nanocrystal

κ = Constant

λ = Wavelength of x-rays

β = Width at half maxima of (111) reflection at Bragg's angle 2θ

θ = Bragg angle

The size of the silver nanoparticle was determined from the line broadening of the (111) reflection using the Debye-Scherrer formula. According to the formula, constant (κ) = 0.94 and wavelength (λ) = 1.5406 × 10<sup>-10</sup>.

## RESULTS

### Synthesis and characterization of copper and zinc nanoparticles

**UV-visible spectroscopy:** The individual UV-vis absorption spectra showed specific criteria of recognition based on the spectra' shape and absorption maxima. The optimization of the synthesis was investigated by recording the characteristic UV-vis absorption spectra of the synthesized zinc nanoparticles between 200–800 nm. The results of UV-visible spectroscopy are presented in Table 1. In ZnNPs were recognized by intense peaks at 266, 368, 410, 471, 605, and 664 nm, respectively (Fig. 1). The spectra of neem ZnNPs with maxima at 648 nm. The ZnO spectra were used for comparison. These spectra and the peak intensities can be considered as preliminary, useful, informative criteria for the recognition of the nanoparticles.

**Field Emission Scanning Electron Microscopy (FESEM) analysis:** The ZnNPs synthesized from plant extracts were characterized in terms of morphology, surface, and size distribution. FESEM is the scanning electron microscope, which forms different images by targeting a high-energy beam of electrons on the surface of a sample and detecting the signals obtained from the interaction of the incident electron with the sample's surface. The FESEM images provide a 3D appearance which is useful for understanding the morphology of the nanoparticles. The results of FESEM depicted the formation of ZnNPs which were well dispersed and the aggregation of the particles could be seen. It indicated that the diameters of ZnNPs in the solution have sizes of several nm which ranged between 181.34-231.64 nm with a predominant shape cluster (Table 2 and Fig. 2). The size of nanoparticles was variable because of the encapsulation and aggregation of nanoparticles by bio-molecules present in the extract.

**Fourier Transform Infrared Spectroscopy (FTIR):** Whereas, FTIR spectra of neem ZnNPs resulted in sharp absorption peaks at 3412.80, 2428.71, 2331.93, 2026.69, 1384.54, 1271.24, 872.47, 444.24 cm<sup>-1</sup> wave number (number of wavelengths per unit distance) (Fig. 3), respectively. Therefore, sharp peaks obtained

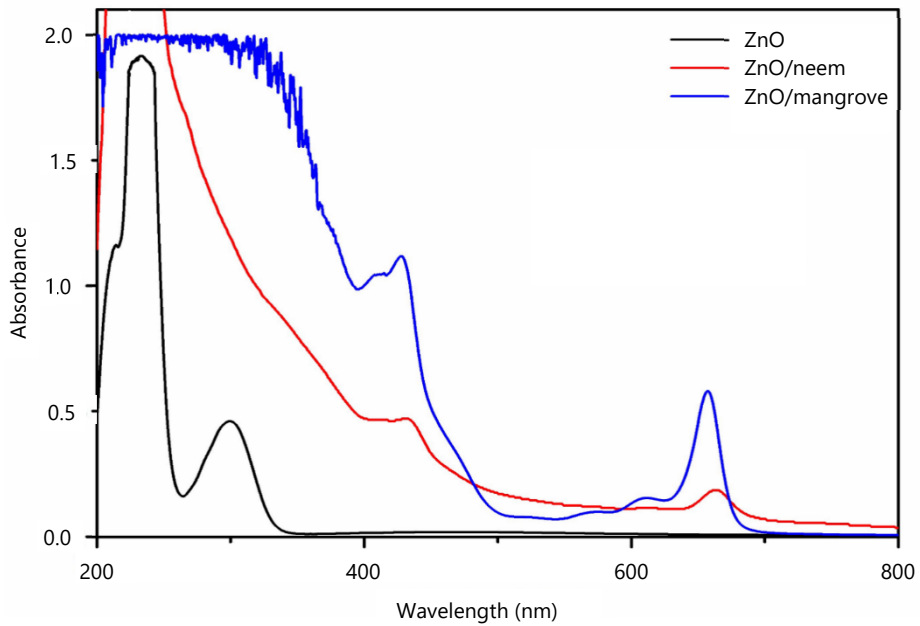


Fig. 1: UV-visible spectroscopy observation of green synthesized zinc (Zn) nanoparticles

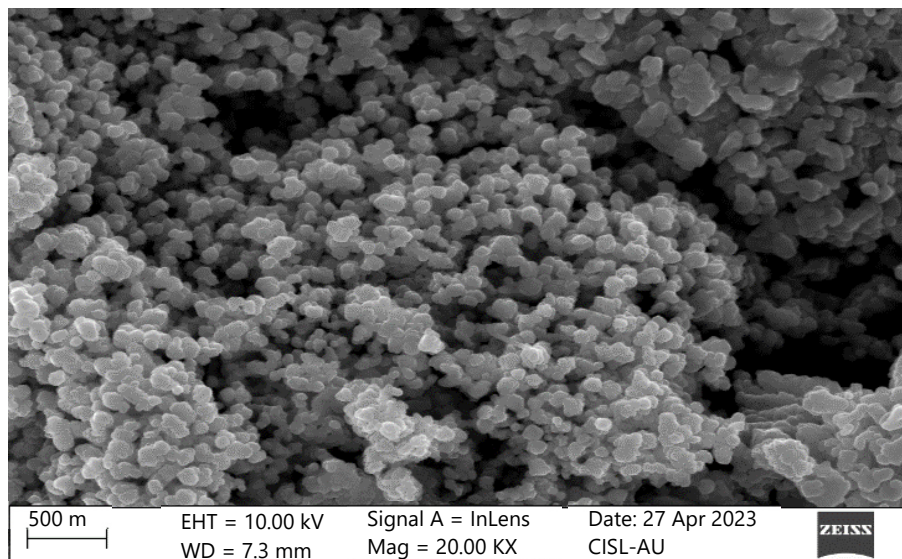


Fig. 2: FESEM observation of neem ZnNPs

Table 1: UV-visible spectroscopy observation of green synthesized zinc nanoparticles

Sample	Wavelength (nm)	Absorbance
ZnO	229	0.94
	233	1.90
ZnO/neem	431	0.95
	648	0.37

Table 2: FESEM results of green synthesized copper and zinc nanoparticles

Nanoparticle	Shape of nanoparticles	Particle size range (nm)	Average size (nm)
Neem ZnNPs	Cluster	181.34 - 231.64	206.49

through FTIR analysis of neem ZnNPs indicated the presence of carboxyl, amide group, and secondary amines which were the main constituents of proteins, which confirmed the strong binding ability of nanoparticles with phytochemicals like phenols, terpenoids, flavonoids and alkaloids etc.

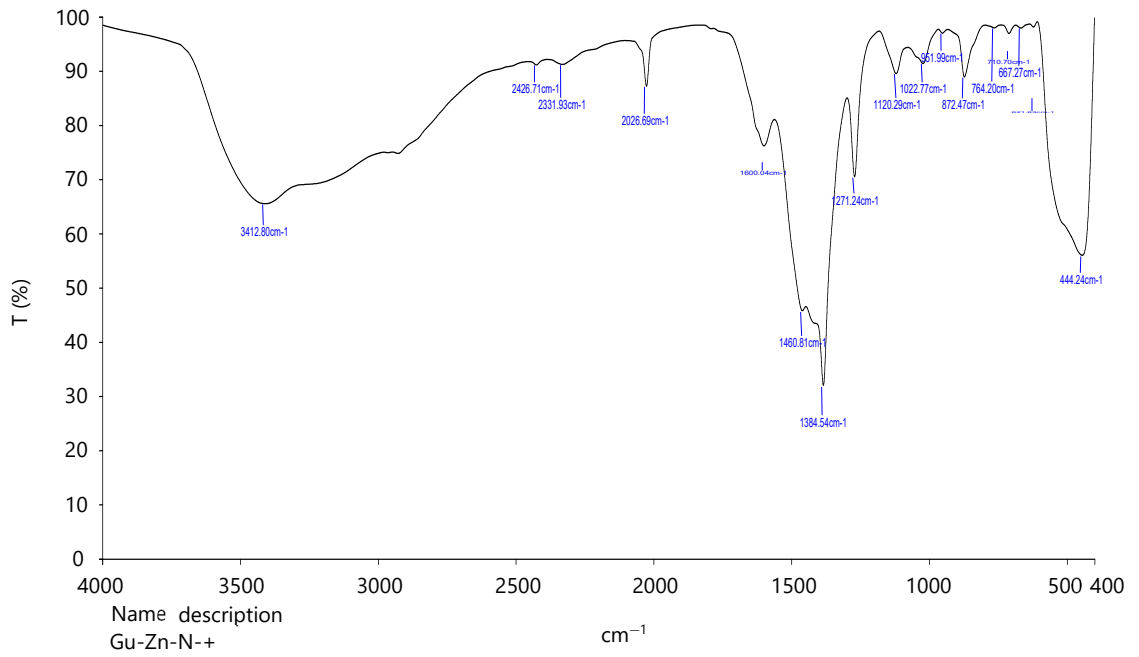


Fig. 3: FTIR analysis of neem ZnNPs

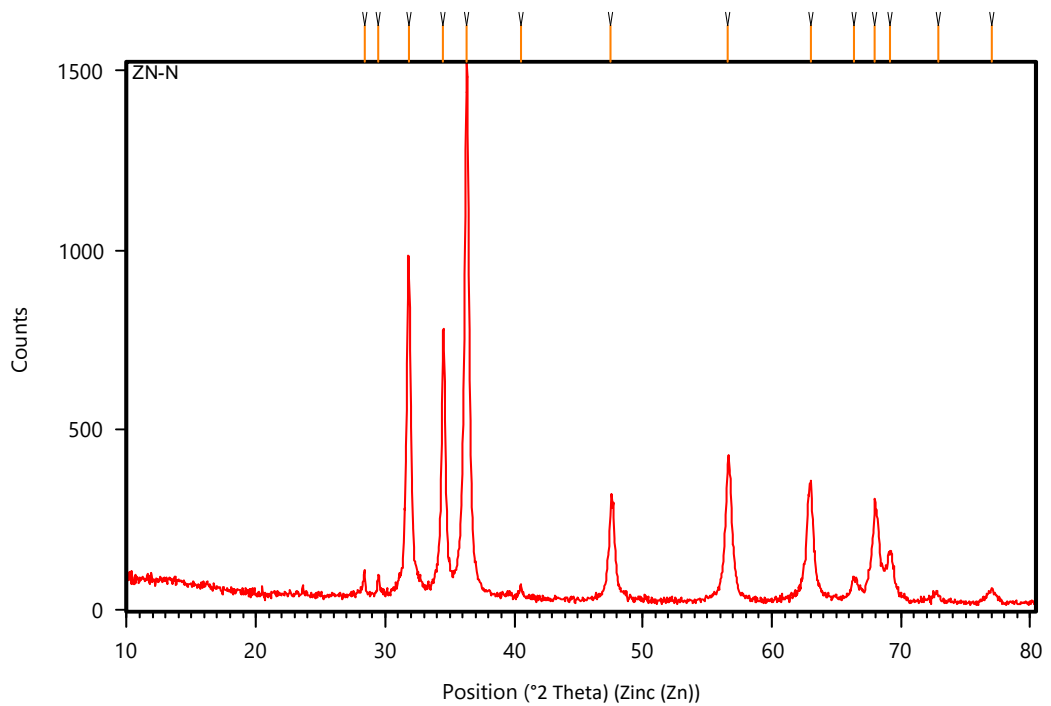


Fig. 4: XRD pattern of neem ZnNPs

Table 3: XRD analysis of green synthesized zinc nanoparticles

Sample	2θ	fwhm	Average (nm)
ZnO/neem	28.3925	0.1181	37.00787
	29.4836	0.1574	
	31.8222	0.2755	
	34.5041	0.2362	
	36.3294	0.2755	
	40.4825	0.3149	
	47.5485	0.3149	

2θ: Angle between transmitted beam and reflected beam and fwhm: Full width at half maximum

**X-ray diffraction (XRD):** The structure and composition of biosynthesized ZnO NPs were further confirmed by X-ray powder Diffraction (XRD) analysis. In the case of neem, ZnNPs peaks observed at  $2\theta = 28.3925, 29.4836, 31.8222, 34.5041, 36.3294, 40.4825,$  and  $47.5485$  were assigned to the (040), (200), (211), (220), (202), (301) and (321) reflection lines respectively. The XRD results for nanoparticles are shown in Fig. 4 and the average crystalline size for neem ZnNPs was calculated by using Debye-Scherrer formula by 37.00 nm (Table 3).

## DISCUSSION

According to Umer *et al.*<sup>11</sup> synthesized copper nanoparticles using ascorbic acid as a reducing agent, similar to the method used in chemical A synthesis. Also Shantkriti and Rani<sup>12</sup> reported parallel results, synthesizing copper nanoparticles using an extract of *Pseudomonas fluorescens* and detecting a specific absorption peak at 610 nm. The absorption spectra of the copper nanoparticles formed during the reaction exhibited a sharp absorbance peak ranging from 550-800 nm<sup>13</sup>.

The capacity of microorganisms to endure and tolerate harmful heavy metals is a prerequisite for the creation of metal and metal oxide nanoparticles. Under stressed conditions, these bacteria can produce metal oxide nanoparticles or other metals by reducing metal ions<sup>14</sup>. Therefore, the natural bio-mineralization process seen in the elevated zinc metal tolerance fungus *Aspergillus aeneus*-which was isolated from an Indian zinc mine and employed in the extracellular synthesis of ZnO nanoparticles-is mimicked by zinc-tolerant microorganisms that produce ZnONPs<sup>15</sup>. Zinc oxide nanoparticles were synthesized environmentally at utilizing a high-purity phycocyanin pigment that is obtained from cyanobacteria<sup>16</sup>. This pigment is highly versatile and may be used in many different sectors. Furthermore, the toxicity of phycocyanin ZnO nanoparticles is reduced due to the protective effect of phycocyanin, which decreases the number of Reactive Oxygen Species (ROS) and makes them suitable for therapeutic use *Catharanthus roseus* leaf extract is rich in alkaloids, phenolic compounds, vincristine, serpentine, and ajmalicine, among other secondary metabolites.

The hexagonal wurtzite ZnO structure's (100), (002), (101), (102), (110), (103), (200), (112) and (201) crystal planes reflected the diffraction peaks seen in the XRD spectrum at particular angles ( $2\theta$ ) of 31, 34, 35, 47, 56, 62, 67, 68 and 69°<sup>17</sup>. The existence of thymol, a well-known phenolic antibacterial compound, was confirmed by the synthesized ZnO nanoparticles' FTIR spectra. Up to 434°C, the TGA/DTA study revealed a 2.4% loss. Up to 10,00°C, no significant loss is seen after this. All that means is that heat causes Zn(OH)<sub>2</sub> to change into ZnO, which is stable above 434°C. Therefore, *Catharanthus roseus* could be a valuable source for the production of ZnO NPs.

A biological approach for the synthesis of zinc oxide nanoparticles using rhamnolipids (RLs) from *Pseudomonas aeruginosa* as efficient stabilizing agents. These nanoparticles exhibited significantly higher antioxidant and free radical scavenging activities indicating their potential as antioxidants in biological systems.

The absorption wavelength at 379 nm of the ZnO NPs indicated their excitonic nature at room temperature as well as the uniform distribution of the nanoparticles<sup>18</sup>. Synthesized ZnO nanoparticles using a zinc-tolerant fungus and observed sharp absorbance at 375 nm and who found a sharp peak at around 364 nm indicating ZnO particle formation<sup>19</sup>. Green synthesized ZnO NPs and recorded a 378 nm SPR peak, which was also reported in close agreement with the research of Selvarajan and Mohanasrinivasan<sup>20</sup>.

The ZnO nanoparticles' UV-visible spectroscopy investigation showed an absorption band with a wavelength of 380 nm, which is within the typical wavelength range of ZnO nanoparticles (350-420 nm)<sup>20</sup>. Additionally, the absence of diffraction peaks from other metal species suggests that ZnO NPs are free

from any other contaminants. The XRD spectrum line extension of diffraction peaks indicates the nanoscale range of the synthesized products. Few researchers of Nazir *et al.*<sup>21</sup> and López-López *et al.*<sup>22</sup> reported similar XRD analysis results that closely align with the findings of the current study. The thermal transition of the Zn-complex produced with various plant extracts was identified using TGA thermograms. The ZnO samples' residual water evaporated, resulting in the weight loss that was seen at temperatures between 78 and 100°C. Weight loss at higher temperatures was ascribed to the loss of own material and the volatilization of phytocomponents found in plant samples. For samples synthesized with *Azadirachta indica*, *Tagetes erecta*, *Lentinula edodes*, *Chrysanthemum morifolium*, and without extract, respectively, a total weight loss at 800°C of 3.28, 2.79, 2.14, 1.96, and 0.97% was estimated<sup>23</sup>.

It is generally believed that the disinfection of microorganisms relies on the direct interaction between nanoparticles and biological cells<sup>21</sup>. The antimicrobial effect of biologically synthesized copper nanoparticles was assessed based on the zone of inhibition.

The antifungal capabilities of ZnONPs against *C. canescens* were evaluated using the agar dilution method. At all test concentrations, the fungal pathogen's radial growth was suppressed to a degree ranging from 35.44 to 89.85%. When CuNPs were administered at concentrations of 1200 and 1500 ppm, respectively, the highest inhibitory activity of 89.85 and 78.65% was noted<sup>23</sup>.

This study effectively synthesized ZnONPs using neem extract but faced some limitations. The particle size was relatively large (149.52-231.64 nm), which may affect their efficiency. The study lacked toxicity assessments, stability tests, and real-world application evaluations. Future research should focus on optimizing synthesis conditions for better size control, conducting comprehensive toxicity studies, and exploring practical applications in agriculture and medicine. Additionally, improving the stability of ZnONPs using capping agents could enhance their effectiveness.

## CONCLUSION

This study focuses on the green synthesis of Zinc Oxide Nanoparticles (ZnONPs) using neem (*Azadirachta indica*) leaf extract. The synthesis involved combining neem extract with zinc salt under controlled stirring conditions, resulting in a color change indicating nanoparticle formation. Characterization techniques such as UV-vis spectroscopy, FESEM, FTIR, and XRD confirmed the presence, size (37 nm), and morphology of the ZnONPs. The nanoparticles exhibited effective antimicrobial properties and potential applications in agriculture and medicine. This eco-friendly approach aligns with sustainable nanotechnology practices.

## SIGNIFICANCE STATEMENT

Environmental concerns surrounding chemical synthesis methods have driven the need for eco-friendly approaches to nanoparticle production. This study successfully synthesized Zinc Oxide Nanoparticles (ZnONPs) using neem leaf extract, confirming their formation through various characterization techniques. The green synthesis method offers a sustainable alternative that reduces harmful by-products and minimizes energy consumption. These ZnONPs have potential applications in agriculture as eco-safe fertilizers and antimicrobial agents, contributing to greener technological advancements. This research underscores the value of plant-based synthesis in promoting environmentally conscious nanotechnology practices.

## REFERENCES

1. Zheng, L., F. Hong, S. Lu and C. Liu, 2005. Effect of nano-TiO<sub>2</sub> on strength of naturally aged seeds and growth of spinach. *Biol. Trace Elem. Res.*, 104: 83-91.
2. Camas, M., F. Celik, A.S. Camas and H.B. Ozalp, 2019. Biosynthesis of gold nanoparticles using marine bacteria and Box-Behnken design optimization. *Part. Sci. Technol.*, 37: 31-38.

3. Nayaka, S., B. Chakraborty, M.P. Bhat, S.K. Nagaraja and D. Airodagi *et al.*, 2020. Biosynthesis, characterization, and *in vitro* assessment on cytotoxicity of actinomycete-synthesized silver nanoparticles on *Allium cepa* root tip cells. Beni-Suef Univ. J. Basic Appl. Sci., Vol. 9. 10.1186/s43088-020-00074-8.
4. Hassan, S.E.D., A. Fouda, A.A. Radwan, S.S. Salem and M.G. Barghoth *et al.*, 2019. Endophytic actinomycetes *Streptomyces* spp mediated biosynthesis of copper oxide nanoparticles as a promising tool for biotechnological applications. J. Biol. Inorg. Chem., 24: 377-393.
5. Imani, M.M. and M. Safaei, 2019. Optimized synthesis of magnesium oxide nanoparticles as bactericidal agents. J. Nanotechnol., Vol. 2019. 10.1155/2019/6063832.
6. Nasrollahzadeh, M., M. Atarod, M. Sajjadi, S.M. Sajadi and Z. Issaabadi, 2019. Plant-Mediated Green Synthesis of Nanostructures: Mechanisms, Characterization, and Applications. In: Interface Science and Technology: An Introduction to Green Nanotechnology, Nasrollahzadeh, M., S.M. Sajadi, M. Sajjadi, Z. Issaabadi and M. Atarod (Eds.), Elsevier, Amsterdam, Netherlands, ISBN: 978-0-12-813586-0, pp: 199-322.
7. Koduru, J.R., S.K. Kailasa, J.R. Bhamore, K.H. Kim, T. Dutta and K. Vellingiri, 2018. Phytochemical-assisted synthetic approaches for silver nanoparticles antimicrobial applications: A review. Adv. Colloid Interface Sci., 256: 326-339.
8. Adhikari, T., S. Kundu, A.K. Biswas, J.C. Tarafdar and A.S. Rao, 2015. Characterization of zinc oxide nanoparticles and their effect on growth of maize (*Zea mays L.*) plant. J. Plant Nutr., 38: 1505-1515.
9. Schievano, E., M. Stocchero, E. Morelato, C. Facchin and S. Mammi, 2012. An NMR-based metabolomic approach to identify the botanical origin of honey. Metabolomics, 8: 679-690.
10. Nadagouda, M.N. and R.S. Varma, 2006. Green and controlled synthesis of gold and platinum nanomaterials using vitamin B<sub>2</sub>: Density-assisted self-assembly of nanospheres, wires and rods. Green Chem., 8: 516-518.
11. Umer, A., S. Naveed, N. Ramzan and M.S. Rafique, 2012. Selection of a suitable method for the synthesis of copper nanoparticles. Nano, Vol. 7. 10.1142/S1793292012300058.
12. Shantkriti, S. and P. Rani, 2014. Biological synthesis of copper nanoparticles using *Pseudomonas fluorescens*. Int. Curr. Microbiol. App. Sci. J., 3: 374-383.
13. Divte, P.R., S. Shende, O.M. Limbalkar and R.A. Kale, 2019. Characterization of biosynthesised copper nanoparticle from *Citrus sinensis* and *in-vitro* evaluation against fungal pathogen *Colletotrichum capsici*. Int. J. Chem. Stud., 7: 325-330.
14. Yusof, H.M., R. Mohamad, U.H. Zaidan and N.A. Abdul Rahman, 2019. Microbial synthesis of zinc oxide nanoparticles and their potential application as an antimicrobial agent and a feed supplement in animal industry: A review. J. Anim. Sci. Biotechnol., Vol. 10. 10.1186/s40104-019-0368-z.
15. Jain, A.K., K. Thanki and S. Jain, 2013. Co-encapsulation of tamoxifen and quercetin in polymeric nanoparticles: Implications on oral bioavailability, antitumor efficacy, and drug-induced toxicity. Mol. Pharmaceutics, 10: 3459-3474.
16. Davaeifar, S., M.H. Modarresi, M. Mohammadi, E. Hashemi and M. Shafiei *et al.*, 2019. Synthesizing, characterizing, and toxicity evaluating of Phycocyanin-ZnO nanorod composites: A back to nature approaches. Colloids Surf., B: Biointerfaces, 175: 221-230.
17. Yang, Y., H. Chen, B. Zhao and X. Bao, 2004. Size control of ZnO nanoparticles via thermal decomposition of zinc acetate coated on organic additives. J. Cryst. Growth, 263: 447-453.
18. Zhang, L., Y. Ding, M. Povey and D. York, 2008. ZnO nanofluids-A potential antibacterial agent. Prog. Nat. Sci., 18: 939-944.
19. Mohammadian, M., Z. Es'haghi and S. Hooshmand, 2018. Green and chemical synthesis of zinc oxide nanoparticles and size evaluation by UV-vis spectroscopy. J. Nanomed. Res., 7: 52-58.
20. Selvarajan, E. and V. Mohanasrinivasan, 2013. Biosynthesis and characterization of ZnO nanoparticles using *Lactobacillus plantarum* VITES07. Mater. Lett., 112: 180-182.

21. Nazir, S., M. Zaka, M. Adil, B.H. Abbasi and C. Hano, 2018. Synthesis, characterisation and bactericidal effect of ZnO nanoparticles via chemical and bio-assisted (*Silybum marianum in vitro* plantlets and callus extract) methods: A comparative study. IET Nanobiotechnol., 12: 604-608.
22. López-López, J., A. Tejada-Ochoa, A. López-Beltrán, J. Herrera-Ramírez and P. Méndez-Herrera, 2022. Sunlight photocatalytic performance of ZnO nanoparticles synthesized by green chemistry using different botanical extracts and zinc acetate as a precursor. *Molecules*, Vol. 27. 10.3390/molecules27010006.
23. Zhao, R., W. Kong, M. Sun, Y. Yang and W. Liu *et al.*, 2018. Highly stable graphene-based nanocomposite (GO-PEI-Ag) with broad-spectrum, long-term antimicrobial activity and antibiofilm effects. *ACS Appl. Mater. Interfaces*, 10: 17617-17629.